JOURNAL OF APPLIED ELECTROCHEMISTRY 26 (1996) 463–469

Chronoamperometry at channel electrodes: analytical theory of transient behaviour at double electrodes

R. G. COMPTON*, J. J. GOODING, A. SOKIRKO†

Physical and Theoretical Chemistry Laboratory, Oxford University, South Parks Road, Oxford, OX1 3QZ, Great Britain

Received 14 August 1995; revised 4 October 1995

An analytical theory is presented which permits the calculation of transient effects at widely-separated double channel electrodes. In particular the current response of a downstream (detector) electrode to a potential leap at an upstream (generator) electrode is established and theoretical predictions are found to be in excellent agreement with experiments carried out using the oxidation of *N,N,N′,N′*-tetramethyl-phenylenediamine in aqueous solution at a platinum double channel electrode.

1. Introduction

The double-channel electrode, pioneered by Gerischer [1], is a valuable approach to the study of intermediates and products of electrode reactions. The basis of such investigations is as follows. A solution species **A**, passes over the upstream generator electrode where it is oxidatively or reductively transformed to a species **B**:

$$\mathbf{A} \pm ne^- \rightleftharpoons \mathbf{B}$$

The species **B** is then transported to the downstream detector electrode where it is analysed amperometrically, generally via reduction or oxidation back to **A**. The experiment is quantitatively characterized by the so-called 'collection efficiency', N, given by

$$N = |I_{det}/I_{gen}| \quad (1)$$

where I_{gen} and I_{det} are the currents at the generator and detector electrodes respectively. Whilst the variation of the steady-state collection efficiency with electrolyte flow rate has been used to characterize the homogeneous chemistry of **B**, it has recently been pointed out [2, 3] that transient measurements using the double channel geometry can provide additional and unique information if the detector electrode current is monitored as a function of time following a potential leap on the upstream electrode. In particular, the ability to probe the diffusion coefficients of electrogenerated species and also heterogeneous kinetics at solid/liquid interfaces was noted. The latter ability was exploited to characterize the nature of electrolytic processes occurring at the surface of porous silicon electrodes [3].

The aim of this paper is to develop *analytically* the theory of transient behaviour at the double channel electrode; it complements the computational approach to this problem presented elsewhere [2] and is directly applicable for cell geometries and relative electrode placements for which computations are particularly CPU-expensive. The basis of our treatment assumes that the channel flow cell contains an electrode of width d, where d is greater than the depth (height) of the channel, h. This assumption simplifies the transport problem to one of two dimensions, as shown schematically in Fig. 1. Previous analytical work on double channel electrodes has been concerned with the deduction of steady-state collection efficiencies [4, 5] and has assumed the limiting case when the thickness of the diffusion layer is significantly lower than height h of the channel:

$$\frac{V_f h}{D\hat{L}d} \gg 1 \quad (2)$$

where V_f is the volume flow rate, D is the diffusion coefficient of species **B** and $\hat{L}$ is the total characteristic length ($\hat{L} = \hat{l}_{gen} + \hat{l}_{gap} + \hat{l}_{det}$) shown in Fig. 1. When Condition 2 is fulfilled, the velocity near the wall can be linearized [6] – the Lévêque approximation [7] – and analytical solution is facilitated [6]. In the other limiting case when the parameter in the left hand side of Condition 2 is of the order of unity numerical solutions are essential [2, 3, 8, 9]. In the present paper we analyse the case of widely separated electrodes ($\hat{l}_{gap} \gg \hat{l}_{gen}, \hat{l}_{det}$) which is easily experimentally realizable for conventional double electrodes as well as for microelectrode arrangements. In this situation Condition 2 allows us to use the Lévêque approximation in the region of the gap and so obtain *simple analytical expressions* for the detector electrode transient resulting from a potential leap at the upstream electrode, including the time delay of the current I_{det} after switching on I_{gen} and the characteristic slope of the detector electrode chronoamperometric transient. The solution presented is general and not restricted to certain Peclet numbers so that axial diffusion effects are taken into account, where appropriate. Moreover, the precise nature of the upstream

*Author to whom all correspondence should be addressed.
†Present address: Electrochemical Laboratories, Trent University, Peterborough, Ontario, K9J 7B8, Canada.

0021-891X

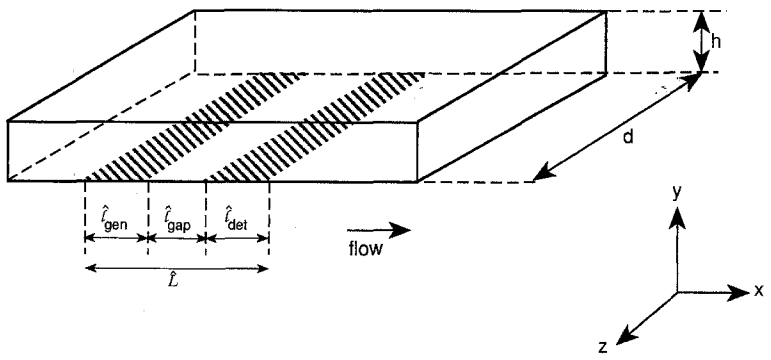

Fig. 1. Schematic diagram of a double channel electrode which defines the coordinate system used and the various cell parameters.

electrode and the reaction there has no influence on the transient collection efficiency which, under the conditions assumed above, is found to be insensitive to the reversible or irreversible nature of the electrode reaction, the applied potential, or the electrode length. Additionally it is shown that the approach can be extended to more complicated systems using, by way of example, the situation when the species **B** undergoes first order homogeneous reactions. Finally some particular cases, where Condition 2 is not applicable, are discussed.

2. Theory

2.1. *Statement of the problem*

The transport process in the double-channel electrode cell can be subdivided into three stages:

(i) Transport of species **A** towards the surface of the generator electrode and then the transport of the product of the electrochemical reaction **B** away from the generator electrode region.
(ii) Transport of **B** through the gap.
(iii) Transport of **B** towards the surface of the detector electrode.

Because the gap is much longer than electrodes ($\hat{l}_{gap} \gg \hat{l}_{gen}, \hat{l}_{det}$), the timescale of the second stage is much greater than of the others. Therefore, two significant simplifications can be made. First, the pertinent convection–diffusion equations can be solved separately for each stage, even if axial (x-direction) diffusion for (i) and/or (iii) is taken into account. Second, the transient behaviour of the system is determined *only* by transport through the gap; we can therefore use steady-state solutions in the vicinity of the two electrodes.

In the following we employ nondimensional variables for length and time, and adopt the notation that the corresponding dimensional parameters will be given a 'hat' as defined below. Thus real time is represented by $\hat{t}$ while t represents dimensionless time. The two parameters are related by the equation $t = \sigma\hat{t}$, where

$$\sigma = \frac{6V_f}{h^2 d} \tag{3}$$

Physically the parameter σ describes the convective flow near the cell wall through the equation $v_x = \sigma\hat{y}$ where v_x is the axial solution velocity through the cell. The quantity $(D/\sigma)^{1/2}$ is used as a measure of distance to create the following dimensionless variables:

$$x = \hat{x}(\sigma/D)^{1/2} \tag{4a}$$

$$y = \hat{y}(\sigma/D)^{1/2} \tag{4b}$$

$$L = \hat{L}(\sigma/D)^{1/2} \tag{4c}$$

$$l_\alpha = \hat{x}_\alpha(\sigma/D)^{1/2} \tag{4d}$$

$$\alpha = (\text{gen, det, gap}) \tag{4e}$$

where the Cartesian coordinates $\hat{x}$ and $\hat{y}$ are defined in Fig. 1. In the above notation the Peclet number, associated with the length $\hat{l}$ is l^2. The concentration of **A** upstream of the generator electrode, $[\mathbf{A}]_{bulk}$, is used to normalise concentrations and a dimensionless current is defined as follows:

$$I = \frac{\hat{I}}{[\mathbf{A}]_{bulk} FD} \tag{5}$$

where F is the Faraday constant.

Subproblem (i), namely, steady state convection–diffusion transport to a channel electrode, has been well studied as follows [12]:

(a) For high Peclet numbers, $l^2 \gg 1$, the classic Lévêque solution is valid [6]:

$$I(l) = \frac{3^{1/3}}{2\Gamma(4/3)} l^{2/3} \qquad l \gg 1 \tag{6}$$

(b) For small Peclet numbers, $l^2 \ll 1$, Ackerberg *et al.* have derived [10] the expression

$$I(l) = \frac{\pi}{\log(4/l) + 1.0559} \qquad l \ll 1 \tag{7}$$

Note that when **A** and **B** have different diffusion coefficients it is appropriate to use D_A in setting up the dimensionless variables in Equations 4 and 5. Otherwise if D_B is selected the right-hand sides of Equations 6 and 7 must be multiplied by the factor (D_B/D_A) for the case of the current flowing at the generator electrode.
(c) For intermediate Peclet numbers, $l^2 \sim 1$, the problem has been solved numerically by Newman [11]. No satisfactory analytical approximations exist [12].

Subproblem (ii) is described by the following convective–diffusion equation written in terms of the dimensionless concentration c ($= [\mathrm{B}]/[\mathrm{A}]_{\mathrm{bulk}}$) of species **B**:

$$\frac{\partial c}{\partial t} = \frac{\partial^2 c}{\partial y^2} - y\frac{\partial c}{\partial x} \tag{8}$$

in the zone $t > 0$, $y > 0$, $x > 0$. The initial and boundary conditions are

$$c = 0 \qquad \text{at } t = 0 \tag{9}$$

$$c = 0 \qquad \text{at } x = 0 \tag{10}$$

$$c = 0 \qquad \text{at } y \to \infty \tag{11}$$

$$\frac{\partial c}{\partial y} = I_{\mathrm{gen}}\delta_+(x) \quad \text{at } y = 0 \tag{12}$$

where $\delta_+(x)$ is the Dirac Impulse function. Boundary conditions 10 and 11 correspond to the absence of species **B** in bulk solution. Boundary condition 12 indicates that the only source of **B** is a generator electrode of small size located at the origin of the coordinate system which, after time $t = 0$, generates a steady current I_{gen}. Solution of the system of equations, Equations 8–12, gives the concentration distribution $c(t, x, y)$ and, in particular, $c(t, L, 0)$ near the electrode.

Solution of subproblem (iii) is analogous to that of subproblem (i). The thickness of the diffusion layer at $x \approx L$ is (assumed) far in excess of the length of the detector electrode so that the detector has no influence on the concentration distribution within the diffusion layer. So, in effect, the detector is situated in a solution of dimensionless concentration $c(t, L, 0)$. Consequently the collection efficiency is

$$N(t, L) = \left| \frac{I(l_{\mathrm{det}})}{I_{\mathrm{gen}}} c(t, L, 0) \right| \tag{13}$$

where $I(l_{\mathrm{det}})$ is given by Equation 6 or 7 as appropriate.

To find the final expression for the transient behaviour of N we next solve Equations 8–12. This is accomplished in the following section.

2.2. *Solution of the transport equation in the gap region*

Double Laplace transformation of Expression 8 first with respect to t (transform variable s) and second with respect to x (transform variable p) gives

$$s\bar{\bar{c}} = \frac{\partial^2 \bar{\bar{c}}}{\partial^2 y} - py\bar{\bar{c}} \tag{14}$$

where $\bar{\bar{c}}$ denotes the double-Laplace transformation of variable c. The solution of Equation 14 which satisfies the boundary and initial conditions, Conditions 9–11, is of the form:

$$\bar{\bar{c}} = \alpha Ai[p^{1/3}(y + s/p)] \tag{15}$$

where $Ai[z]$ denotes the Airy function [13] and the constant α is obtained from Laplace transformation of Equation 12:

$$\frac{\partial \bar{\bar{c}}}{\partial y} = \frac{I_{\mathrm{gen}}}{s} \qquad \text{at } y = 0 \tag{16}$$

Combining Equations 15 and 16, we obtain the concentration distribution at $y = 0$

$$\bar{\bar{c}} = \frac{I_{\mathrm{gen}}}{sp^{1/3}} f[sp^{-2/3}] \tag{17}$$

where

$$f[z] = -\frac{Ai[z]}{Ai'[z]} \tag{18}$$

To find the inverse Laplace transformation of Equation 17 we substitute the Taylor series for $f[z]$. Now from the definition of the Airy function, $Ai''[z] = zAi[z]$, we can obtain

$$f'[z] = zf^2[z] - 1 \tag{19}$$

which allows us to develop the required series:

$$f[z] \approx f[0] + zf'[0] + z^2 f''[0]/2 = f[0] - z + z^2 f^2[0]/2 \tag{20}$$

where

$$f[0] = 3^{1/3}\Gamma(1/3)/\Gamma(2/3) \tag{21}$$

Substituting Equations 20 and 21 into Equation 17 and taking the formal inverse Laplace transformations with respect to time and x, we obtain at $y = 0$:

$$c = \frac{I_{\mathrm{gen}} x^{-2/3}}{3^{1/3}\Gamma(2/3)} - I_{\mathrm{gen}}\delta_+(t) + \frac{I_{\mathrm{gen}}\pi^2 x^{2/3}}{3^{2/3}\Gamma^{2/3}(2/3)}\delta'_+(t) \tag{22}$$

The first term in Equation 22 corresponds to the steady-state concentration. Substituting it into Equation 13 we obtain the steady state current efficiency N_0

$$N_0 = I(l_{\mathrm{det}})\frac{L^{-2/3}}{3^{1/3}\Gamma(2/3)} \tag{23}$$

where $I(l_{\mathrm{det}})$ is given by Equation 6 or Equation 7 as appropriate.

We turn next to the second and third terms in Equation 22 and note that the physical significance of these terms is obscure until Expression 23 has been suitably integrated, as follows. To this end we idealize the detector electrode response by the step-form shown schematically in Fig. 2(a) which is characterized by the point $t = t_0$. The integration of the first two terms of Equation 22 with respect to time gives us the time t_0 when the concentration at first time becomes nonnegative ($c = 0$):

$$t_0 = 3^{1/3}\Gamma(2/3)L^{2/3} \tag{24}$$

The mathematical background to this derives from the time-dependence of the total charge $Q(t) = \int_0^t \mathrm{d}t\, I_{\mathrm{det}}(t)$ passing through the detector electrode which has the form of the smooth curve starting at zero sketched in Fig. 2(b). The two term approximation to Equation 22 gives the straight line to which the

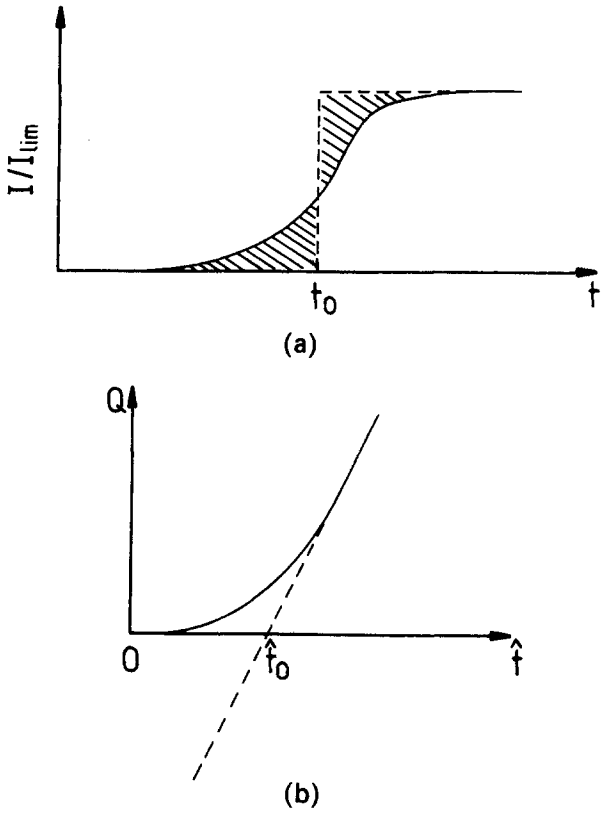

Fig. 2. (a) A schematic detector electrode current transient resulting from a potential step at the generator electrode. (b) The charge flowing at the detector electrode as a function of time and obtained through the integration of the curve shown in Fig. 2(a) and assuming that the shaded zones in that figure are equal in area.

curve in Fig. 2(b) tends at long time $t \gg 1$; from this the value of t_0 is readily deduced.

To investigate the shape of the curve $I_{det}(t)$ quantitatively we idealize the transient by the form shown in Fig. 3 in which the current I_{det} is zero up to time t_1, then changes linearly to the steady state value, which is attained at time t_2. Note that this approximation is characterized by three parameters: the steady state current, the time delay t_0 and the rate of current change (transient slope) near $t = t_0$. We integrate Expression 22 twice with respect to time to obtain for $x = L$

$$\int_0^t \mathrm{d}t \int_0^t \mathrm{d}t\, c(t) = \frac{I_{gen} x^{-2/3}}{3^{1/3}\Gamma(2/3)} \frac{t^2}{2} - I_{gen} t + \frac{I_{gen} \pi^2 x^{2/3}}{3^{2/3}\Gamma^{2/3}(2/3)} \tag{25}$$

For comparison the test curve (Fig. 3) is also integrated twice. The initial segment $0 < t < t_1$ is unchanged by this operation, while the straight line $t > t_2$ becomes part of the parabola in Equation 25.

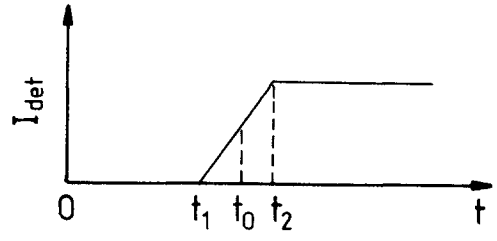

Fig. 3. The idealised transient used to model the schematic experimental transient shown in Fig. 2(a).

The segment between points t_1 and t_2 is transformed into a cubic curve, which meets the already identified curves at the points t_1 and t_2. Moreover, at the points $t = t_1$ and $t = t_2$ the derivatives and the second derivatives of the function given in Equation 25 must be continuous. These six conditions give us a system of algebraic equations which can be solved to give the following simple expression for the chronoamperometric curve between points t_1 and t_2:

$$I_{det}(t) = I_{det}(t \to \infty)\left[\frac{1}{2} + \frac{t/t_0 - 1}{\sqrt{27\Gamma^{1/3}(1/3)\pi^{-4}/8 - 12}}\right] \tag{26}$$

Expression 26 is valid only while the term in the square brackets in the right side is within the interval between 0 and 1.

2.3. *Theoretical results and discussion*

The time dependence of the collection efficiency, N, after calculation of the constants in Expressions 22, 24 and 26 is

$$N = N_0 \begin{cases} 0 & \text{at } 0 < t < 0.55\, t_0 \\ 1.1131\, t/t_0 - 0.6131 & \text{at } 0.55\, t_0 < t < 1.45\, t_0 \\ 1 & \text{at } t > 1.45\, t_0 \end{cases} \tag{27}$$

where t_0 is the time when N reaches half of its steady state value,

$$t_0 = 1.9553\, L^{2/3} \tag{28}$$

and N_0 is the steady state collection efficiency

$$N_0 = 0.5114\, L^{-2/3} I(l_{det}) \tag{29}$$

In the two limiting cases of high and small Peclet numbers Expression 29 can be simplified, taking into account either Equation 6 or 7, that is,

$$N_0 = \frac{3\sqrt{3}}{4\pi}\left(\frac{l_{det}}{L}\right)^{2/3} \approx 0.4135\left(\frac{l_{det}}{L}\right)^{2/3} \qquad l_{det} \gg 1 \tag{30}$$

$$N_0 = \frac{1.607\, L^{-2/3}}{2.442 - \log l_{det}} \qquad l_{det} \ll 1 \tag{31}$$

Expressions 27–31 are given in dimensionless form. It is, however, useful to consider how they depend on various experimental parameters. First, the concentration in the diffusion layer and I_{det} are both proportional to the current flowing at the generator electrode. It follows therefore that the collection efficiency does not depend on a size of the generator electrode, the reversibility of reaction on it, the bulk concentration of substance **A**, or its diffusion coefficient D_A. These features follow directly from the assumption $l_{gen} \ll l_{gap} \approx L$. For a Peclet number $l_{det}^2 \gg 1$ it is possible to neglect axial diffusion in the vicinity of the detector electrode and the steady state collection efficiency N_0 depends only on the ratio of

the detector electrode length l_{det} and the gap length $l_{gap} \approx L$. Under these conditions it is independent of the solution flow rate and or the diffusion coefficient. We note that Expression 30 can be obtained as a limiting case of Matsuda's results [4] for $l_{det} \ll L$. In the opposite case of a very short detector electrode $l_{det}^2 \ll 1$ N_0 becomes independent on the absolute values of both L and l_{det} as given in Equation 31.

The time for the current I_{det} to reach half of its steady state value is given by the simple equation, Equation 28. According to this expression, the value of t_0 does not depend on the length of the detector electrode or on details of the electrode kinetics on the detector electrode. In dimensional form it becomes

$$\hat{t}_0 = 1.9553\left(\frac{h^2 d\hat{L}}{6V_f}\right)^{2/3} D^{-1/3} \qquad (32)$$

The only unknown parameter in Equation 32 is the diffusion coefficient D of species **B**. Transient collection efficiency experiments may therefore be used to estimate this parameter [3]; the above theory permits the deduction of this quantity without resort to computational modelling of the full transient as previously required and which is timewise prohibitively expensive in the case of widely separated electrodes [2, 3].

Finally, Equation 27 shows that the detector electrode jumps from zero current to its steady-state value rather sharply: the period of the transient behaviour occurs within 90% of t_0. Moreover, since this value of 90% is fixed for any system, it implies that, after renormalization by appropriate values of N_0 and t_0, all transients, $N(t)$, are approximately identical. This procedure is experimentally valuable as a check on the applicability of the present theory – which requires $l_{gap} \gg l_{det}, l_{gen}$ and the absence of homogeneous reactions – to any real system.

The technique of analytical solution developed in this paper is readily extended to some related problems. For example, consider the problem of the steady-state collection efficiency in a system where the substance **B** undergoes first order homogeneous decomposition into an electroinactive species. The convective–diffusion equation for such a system is

$$kc = \frac{\partial^2 c}{\partial y^2} - y\frac{\partial c}{\partial x} \qquad (33)$$

where k is the dimensionless rate constant for the reaction: $k = \hat{k}/\sigma$.

To solve Equation 33 with the boundary and initial conditions (9–12) we Laplace transform with respect to the coordinate x only (transform variable p) to obtain what is effectively Equation 14, except that the variable s is now replaced by k. The transformed boundary condition (Equation 12) becomes $\partial\bar{c}/\partial y = I_{gen}$ at $y = 0$ and Laplace transformation for the concentration at $y = 0$ gives

$$\bar{c} = I_{gen} p^{-1/3} f[sp^{-2/3}] \qquad (34)$$

Substituting the approximate expression (Equation 20) for $f[z]$ into Equation 34 and taking the inverse Laplace transformation, we obtain the final expression for the collection efficiency in a form very similar to Equation 22:

$$N_2 = I_{det}\left[\frac{L^{-2/3}}{3^{1/3}\Gamma(2/3)} - k + \frac{\pi^2 L^{2/3}}{3^{2/3}\Gamma^{2/3}(2/3)}k^2\right] \qquad (35)$$

The subscript 2 on N_2 denotes that terms in the expansion of $f[z]$ were taken into account up to and including the second power. Note that the first term in the right-hand side of Equation 34 is N_0. Equation 35 provides a basis for the experimental estimation of k. In the case of slow reactions, $(k/L^{2/3}) \ll 1$, and the last term in the equation can be omitted so that

$$\hat{k} = 0.5114\left(\frac{6V_f}{h^2 d\hat{L}}\right)^{2/3} D^{1/3}\frac{N_0 - N_2}{N_0} \qquad (36)$$

This expression allows us to find $\hat{k}$ provided the diffusion coefficient of **B** is known, for example from data for t_0.

Finally, we consider the situation when Condition 2 breaks down, that is when the thickness of the diffusion layer becomes comparable with half-height of channel as happens at very slow flow rates. For sufficiently slow flow, $V_f h \ll D\hat{L}d$, and so-called thin-layer conditions operate such that the steady-state concentration of **B** is uniform throughout the channel and depends only on I_{gen} and the channel size h:

$$c = I_{gen}/(h\sqrt{\sigma/D})$$

The collection efficiency N_0 may then be calculated from

$$N_0 = 0.5114\left(\frac{dD}{6V_f}\right)^{1/2} I(l_{det}) \qquad (37)$$

instead of Equation 29.

3. Experimental details

The channel flow cell and flow system have been described in full detail previously [13, 14]. In brief, experiments were carried out in a flow cell fabricated in perspex such that the channel was 6 cm long, 0.6 cm wide and approximately 0.1 cm deep. The exact depth of the cell was determined from a plot of the transport limited current versus (flow rate)$^{1/3}$ for the one-electron oxidation at the generator electrode of TMPD which has a known diffusion coefficient 6.3×10^{-6} cm^{-2} s^{-1} [15]. The cell coverplate bore the generator and detector electrodes which were constructed from strips of platinum foil (99.95%, Goodfellows, Cambridge, UK) 0.0255 mm thick. The electrodes were cemented to the coverplate using

Table 1. Dimensions of the cell used in the double channel experiments

Generator electrode	Length 0.107 cm, width 0.417 cm
Gap length	1.386 cm
Detector electrode	Length 0.112 cm, width 0.423 cm
Cell height	0.0882 cm
Channel width	0.600 cm

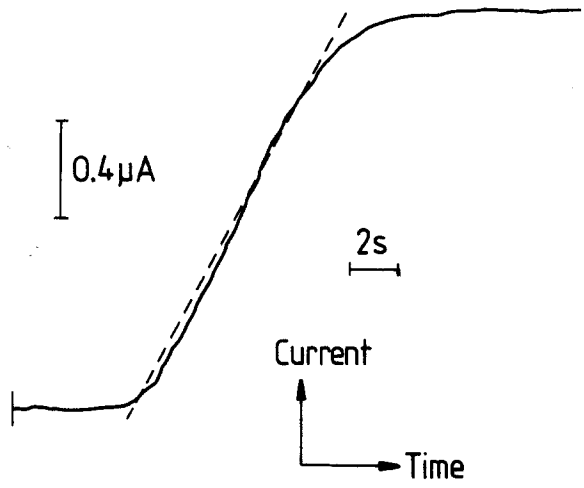

Fig. 4. An experimental detector electrode transient measured using a flow cell of the geometry specified in Table 1 and the flow rate given in the text.

Araldite. Before use the electrodes were polished to a mirror finish using progressively finer diamond lapping compounds (Engis, Maidstone). The smallest diamond grit used was 0.25 μm. The dimensions of the electrodes and the gap between then were measured with a travelling microscope (see Table 1). The channel cell was formed by clamping the coverplate over the channel. A silver wire pseudo-reference electrode was locate upstream of the channel and a platinum gauze counter electrode was situated immediately downstream.

Solution deoxygenated with argon was gravity fed to the cell from a glass reservoir via several metres of 1.5 mm bore glass tubing. Flow rates over a wide range (10^{-4} to 10^{-1} cm^3 s^{-1}) were attained by switching between capillaries with different internal bores and by varying the height of the reservoir relative to the cell outlet. The cell and approximately 1 m of tubing were located in an air thermostatted box at 25 ± 0.5 °C.

TMPD was supplied by Aldrich (Gillingham, UK, 98%) and KCl by BDH (Poole, UK, AnalaR). Solutions were made up with Elgastat (High Wycombe, Bucks) UHQ grade water with a resistivity not less than 18 MΩ cm.

4. Experimental results and discussion

Double channel experiments were conducted using 4×10^{-3} M *N,N,N′,N′*-tetramethyl-*p*-phenylenediamine (TMPD) in aqueous solution containing 0.2 M KCl. Both the detector and generator electrodes were constructed from platinum at which TMPD is known [15] to undergo a reversible one-electron oxidation to a stable radical cation.

Experiments were conducted in which the potential of the generator electrode was stepped from a value at which no current flowed (−0.20 V vs Ag) to one corresponding to the transport limited oxidation of TMPD (0.26 V vs Ag):

$$\mathrm{TMPD} - \mathrm{e}^- \rightleftharpoons \mathrm{TMPD}^{+\cdot}$$

The detector electrode potential was held throughout at a potential of −0.13 V (vs Ag) corresponding to the transport controlled reduction of the radical cation, $\mathrm{TMPD}^{+\cdot}$, back to the parent TMPD. A typical detector electrode transient is shown in Fig. 4 which relates to a flow rate of 0.0412 cm^3 s^{-1}. The time, t_0, for the transient to reach half of its steady-state value was recorded as a function of flow rate and the dependence of t_0/s on the volume flow rate, V_f/cm^3 s^{-1} is shown in Fig. 5 where the x-axis is $V_f^{-2/3}$ as suggested by Equation 32. The excellent linear correlation shown is exactly as predicted theoretically. Moreover, using the known value for the diffusion coefficient of TMPD, $D = 6.3 \times 10^{-6}$ cm^2 s^{-1}, [15] the slope of the plot shown in Fig. 5 is predicted to be 1.23 from Equation 32 if $\hat{L}$ is intepreted as the distance between the middle of detector and generator electrodes.

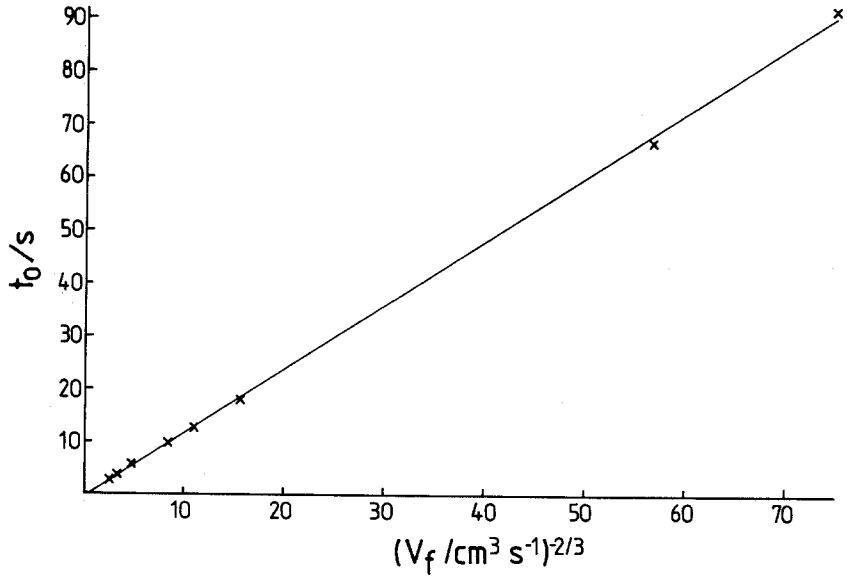

Fig. 5. Analysis of experimental detector electrode transients according to the Equation 26.

The value obtained by fitting a least squares slope to the data shown was 1.21 which is in excellent agreement with the theoretical prediction.

We next return to the illustrative experimental detector current transient shown by the solid line in Fig. 5. It is interesting to compare the shape of this with that predicted by the simplified theory summarized in Equation 26. This is shown as the dashed line in Fig. 5. The theoretical line is seen to be in very good agreement with experiment. Moreover, the experimental transient is seen to be closely symmetrical about the point t_0 (as centre of inversion) so that the approximation $I(t_0) = 0.5\,I(t \rightarrow \infty)$ is seen to be an adequate operational definition of the point t_0, which is strictly defined in Fig. 2(b).

5. Conclusions

The analytical theory developed is seen to be in excellent agreement with experimental measurements made at widely separated double channel electrodes. The simple relationships given in Equation 27 should facilitate the easy analysis of experimental transient data without the need for computational modelling.

References

[1] H. Gerischer, I. Mattes and R. Braun, *J. Electroanal. Chem.* **10** (1965) 553.
[2] R. G. Compton, B. A. Coles and A. C. Fisher, *J. Phys. Chem.* **98** (1994) 2441.
[3] R. G. Compton, B. A. Coles, J. J. Gooding, A. C. Fisher and T. I. Cox, *J. Phys. Chem.* **98** (1994) 2446.
[4] H. Matsuda, *J. Electroanal. Chem.* **16** (1968) 153.
[5] R. Braun, *ibid.* **19** (1968) 23.
[6] P. R. Unwin and R. G. Compton, *Comp. Chem. Kinetics* **29** (1989) 173.
[7] M. A. Lévêque, *Ann. Mines Mem. Ser. 12* **13** (1928) 201.
[8] R. G. Compton, A. C. Fisher, R. G. Wellington, P. J. Dobson and P. A. Leigh, *J. Phys. Chem.* **97** (1993) 10410.
[9] R. G. Compton, R. A. W. Dryfe, J. A. Alsden, N. V. Rees, P. J. Dobson and P. A. Leigh, *ibid.* **98** (1994) 1270.
[10] R. C. Ackerberg, R. D. Patel and S. K. Gupta, *J. Fluid Mech.* **86** (1978) 49.
[11] J. Newman, *Electroanal. Chem.* **6** (1973) 187.
[12] T. J. Pedley, 'The Fluid Mechanics of Large Blood Vessels', Cambridge Monographs on Mechanics and Applied Mathematics, Cambridge (1980).
[13] M. Abramowitz and I. A. Stegun, 'Handbook of Mathematical Functions', Dover Publications, New York (1972), p. 446.
[14] R. G. Compton and P. R. Unwin, *Phil. Trans. R. Soc. Lond.* **A330** (1990) 1.
[15] R. G. Compton, G. M. Stearn, P. R. Unwin and A. J. Barwise, *J. Appl. Electrochem.* **18** (1988) 657.
[16] R. G. Harland and R. G. Compton, *J. Coll. Interface Sci.* **131** (1989) 83.